

3-D SPATIOTEMPORAL SUBBAND DECOMPOSITION OF IMAGE SEQUENCES BY MATHEMATICAL MORPHOLOGY

Soo-Chang Pei¹ and Fei-Chin Chen²

¹Department of Electrical Engineering
National Taiwan University
Taipei, Taiwan, Rep. of China

²Department of Electrical Engineering
National Taiwan Institute of Technology
Taipei, Taiwan, Rep. of China

Abstract: An efficient 3-D spatiotemporal image sequence decomposition method using mathematical morphology is described in this paper; it decomposes the input signal spectrum into 8 spatiotemporal subband images by using two different sets of structuring elements respectively; then each band image can be decimated and coded effectively for data transmission. This subband pyramid scheme preserves the number of pixels as in the original image, has efficient hierarchical data structure, and also allows parallel implementation. Therefore, this scheme has great potential for High Definition Television (HDTV) coding and multimediu video compression, etc. Meanwhile, the unique advantages of morphology over linear filtering approach are its direct geometric interpretation, simplicity and efficiency in parallel/pipelining hardware implementation. Some image sequence examples are given to show the effectiveness of this approach.

I. INTRODUCTION

Subband coding is a very promising source coding scheme, which is widely used for speech compression [1], 2-D video coding [2][3] and 3-D image sequence coding [4][5][6] etc. It decomposes the input signal into several narrowbands that are decimated and encoded separately, encoding of each subbands will be performed according to the statistics of each signal.

The major concern on subband coding scheme is the hardware complexity, design constraint and speed requirement of the linear quadrature mirror filters in the filter banks. An efficient 2-D subband image decomposition using mathematical morphology has been proposed recently to overcome these problems by the authors. The major advantages of morphological approach over the conventional linear filtering approach are their direct geometric interpretations, data structure simplicity and pipelining efficiency in hardware implementation [8].

This paper extends to 3-D spatiotemporal subband decomposition for image sequences using mathematical morphology, since morphological opening and closing provide very good smoothing results as shape filter, also the morphological operations involved are very simple, fast and well suitable for VLSI implementation.

II. 3-D SPATIOTEMPORAL 4 BY 2 EIGHT SUBBAND FOR IMAGE SEQUENCES USING MORPHOLOGICAL FILTERS

In 3-D subband coding system, the digital video signal is filtered and sub-sampled in all three dimensions (temporally, horizontally and vertically) to yield the subbands, from which the input signal can be perfectly reconstructed. Consider the 3-D spatiotemporal 8 subband image coder shown in Fig.1 and 2; During the analysis stage, the incoming signal is filtered into eight subband components, each of which is decimated and encoded for transmission. At the reconstruction stage, the channel signals are decoded, interpolated and recombined to form the reconstructed signal. Now the morphological lowpass filters are used here instead of the conventional linear quadrature mirror filters. The 3-D spatiotemporal analysis/synthesis filter banks can be designed by a separable product of 1-D horizontal and vertical spatial morphological filters with 1-D temporal morphological filter. This will give rise to an analysis of the image sequences into eight bands (Fig.1) as below:

Horizontal	Vertical	Temporal	Band
Low	Low	Low	000
Low	Low	high	001
Low	High	Low	010
Low	High	High	011
High	Low	Low	100
High	Low	High	101
High	High	Low	110
High	High	High	111

With mathematical morphology filter technologies, the complexity of filter design and implementation is greatly reduced. Also mathematical morphology can provide a unique geometric representation of an image by summarizing its shape and conveying its size, orientation and connectivity.

Sequential alternating application of the morphological operations of opening and closing by means of the same structuring element removes details of the image that are small relative to this structuring element. These alternating sequential filters are called morphological low-pass filters. The 1-D high-pass filters can be constructed with the original signal X and the complement of the low-pass filtering $[-H_0(X)]$ as follows:

1-D low-pass analysis filter H_0 :
closing[opening(X)] (1)

1-D high-pass analysis filter H_1 :
 $X-H_0(X)$ (2)

1-D low-pass synthesis filter F_0 :
dilation(Y) (3)

1-D high-pass synthesis filter F_1 :
 $Y-F_0(Y)$ (4)

Then 3-D analysis/synthesis filter banks in an eight-subband coder can be designed by a separable product of the above 1-D horizontal, vertical and temporal morphological filters, for example

3-D low-high-low analysis filter H_{010} :
 $H_0^t\{H_1^v[H_0^h(X)]\}$ (5)

3-D high-high-low synthesis filter F_{110} :
 $F_0^t\{F_1^v[F_1^h(Y)]\}$ (6)

where $H_1^h(F_1^h)$, $H_1^v(F_1^v)$ and $H_1^t(F_1^t)$ for $i=0,1$ are the horizontal, vertical and temporal low/high-pass filters, respectively. Also, the low-pass filter and its complementary high-pass filter can be implemented by only one sequential opening and closing operation with a one-input/two-output scheme.

The system diagrams of 4x2 spatiotemporal subband splitting using morphological filters shown in Figs.3(a) and (b). As shown in Fig.1 the three dimensional subband analysis system consists of spatial (horizontal and vertical) and temporal filtering. In Fig. 3(b), first every frame of the original image sequence is decomposed into four spatial subbands by spatial horizontal/vertical morphological analysis filter banks, each subband is sub-sampled by a factor of four, and then four subband images are combined into a frame for efficient storage and processing. Then the resultant image sequences are decomposed again into two temporal subbands by temporal low/high morphological analysis filter banks. Consequently this image sequences split into two image sequences corresponding to low and high temporal frequency subbands. Finally the two image sequences are sub-sampled in temporal direction by a factor of two. This sub-sampling operation is simply achieved by frame skipping. Notice that the filter bank has another advantage in terms of implementation, because the video signals are decimated after filtering, the filter banks acts as a demultiplexer and the final encoding processing at each subband occurs at only one eighth of the original video input rate. This reduced rate operation is very attractive for high speed HDTV coding and hardware implementation.

III. EXPERIMENTAL RESULTS

The image sequences "Salesman" used in our experiments are shown in Fig.4 with frame size 288x360. We have used a 1x3 horizontal structuring element, a 3x1 vertical structuring element and a 1x3 temporal direction structuring element for 3D spatiotemporal 4x2 subband image sequence decomposition. The experimental results are shown in

Figs.5, 6, and 7. The lowest band analysis images $y_{000}^0(m,n,t)$ and $y_{000}^{14}(m,n,t)$ in Fig.5 contain the most information and give the general brightness of the picture, where the superscript 0 and 14 indicate the frame numbers in the image sequences. For the temporally low band images as shown in Figs.5(a) and (c), the horizontal band and vertical band analysis images $y_{100}^0(m,n,t)$, $y_{100}^{14}(m,n,t)$ and $y_{010}^0(m,n,t)$, $y_{010}^{14}(m,n,t)$ have successfully extracted the vertical and horizontal sharp edges respectively, and the diagonal band analysis images $y_{110}^0(m,n,t)$ and $y_{110}^{14}(m,n,t)$ show the diagonal edges of the pictures. Generally all the above temporally low band images contain the nearly stationary information of the images in each band. On the other hand, the temporally high band analysis images in Figs.5(b) and (d): $y_{001}^i(m,n,t)$, $y_{011}^i(m,n,t)$, $y_{101}^i(m,n,t)$, $y_{111}^i(m,n,t)$ for $i=0, 14$ have successfully extracted the moving status of the "Salesman" image sequences. Fig.(6) shows the four spatial subband synthesis images at the last stage of 4x2 subband reconstruction i.e. $\hat{r}_{00}^0(m,n,t)$, $\hat{r}_{01}^0(m,n,t)$, $\hat{r}_{10}^0(m,n,t)$ and $\hat{r}_{11}^0(m,n,t)$ for number 0 image in the "Salesman" image sequence. These four images are combined into the final reconstructed image $\hat{x}^0(m,n,t)$ shown in Fig.7(a), and the error image in Fig.7(b) gives the reconstruction localization error of the small picture details relative to the size of the structuring element. The SNR of the reconstructed image $\hat{x}^0(m,n,t)$ to the original image $x^0(m,n,t)$ in 3-D spatiotemporal 4x2 subband decomposition is 23.35dB.

V. CONCLUSIONS

This paper has described efficient 3-D spatiotemporal subband decomposition methods using mathematical morphology. These subband decomposition schemes preserve the number of pixels, have efficient hierarchical data structure, and also allow parallel/pipeline implementation. Also the morphological operations involved are very simple, fast and well suitable for VLSI implementation. Some image sequence examples are given to show the effectiveness of this approach.

REFERENCES

- [1] R.E. Crochiere, S.A. Webber and J.L. Flanagan, "Digital coding of speech in subbands", Bell Syst. Tech. J. Vol.55, No.8, pp.1069-1085, Oct. 1976.
- [2] J.W. Woods and S.D. O'Neil, "Sub-band coding of images," IEEE Trans. Acoust Speech, Signal Processing, Vol.ASSP-34, No.5, pp.1278-1288, Oct. 1986.
- [3] H. Gharavi and A. Tabatabai, "Subband coding of monochrome and color images," IEEE Trans. Circuits, Syst., Vol.CAS-35, pp.207-214, Feb. 1988.

- [4] G. Karlsson and M. Vetterli, "Three dimensional subband coding of video," Proc. of IEEE Int'l Conf. on ASSP, New York, pp.1100-1103, Apr. 1988.
- [5] D. LeGall, H. Gaggioni and C.F. Chen, "Transmission of HDTV signals under 140 Mbits/s using a sub-band decomposition and discrete cosine transform coding," Proc. of Signal Processing of HDTV, L Chiariglione, ed. Amsterdam Netherlands, North-Holland pp.287-293, March 1988.
- [6] J.W. Woods and T. Naveen, "Subband encoding of Video Sequences," Proc. of SPIE Conf. on Visual Communications and Image Processing, Philadelphia, PA, pp.724-732, Nov. 1989.
- [7] S.C. Pei and F.C. Chen, "Subband decomposition of monochrome and color images by mathematical morphology," Optical Engineering, Vol.30, No.7, Special Section on Visual Communication and Image Processing III, pp.921-933, July 1991.
- [8] R.M. Haralick and X. Zhuang, "Pipeline architectures for morphological image analysis," Machine Vision and Applications Vol.1, pp.23-40, 1988.

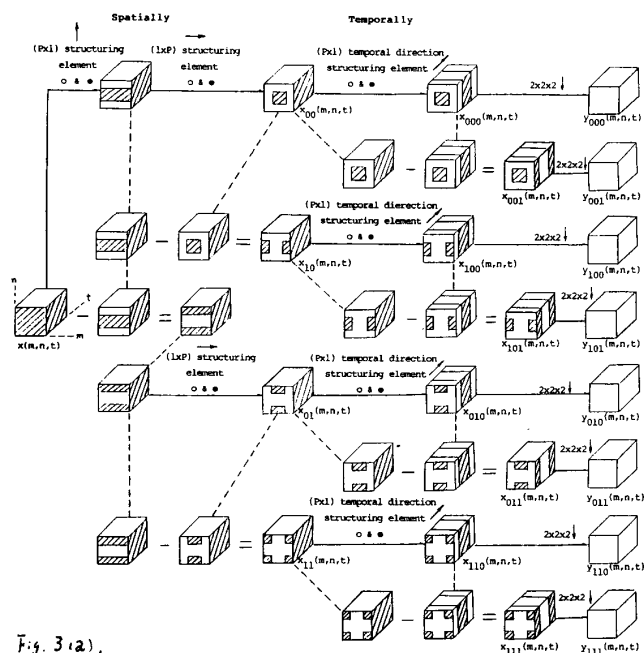


Fig. 3(a).

System Diagram of 4x2 Spatiotemporal Subband Splitting Using Mathematical Morphology Analysis Filter Banks.

- The passband/stopband are located in the shaded/blank area
- The same data are shared and indicated by the dash lines.

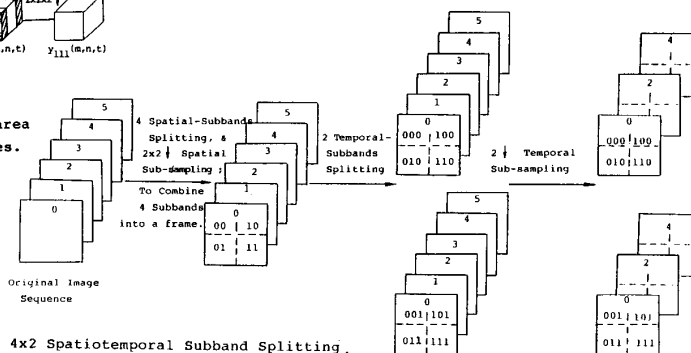


Fig. 3(b).

Flow Diagram of 4x2 Spatiotemporal Subband Splitting.

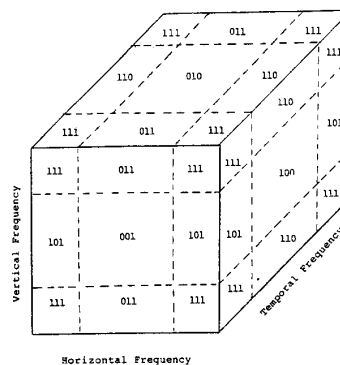


Fig. 1.

Ideal 8-Band Splitting in 3D Subband Coder.

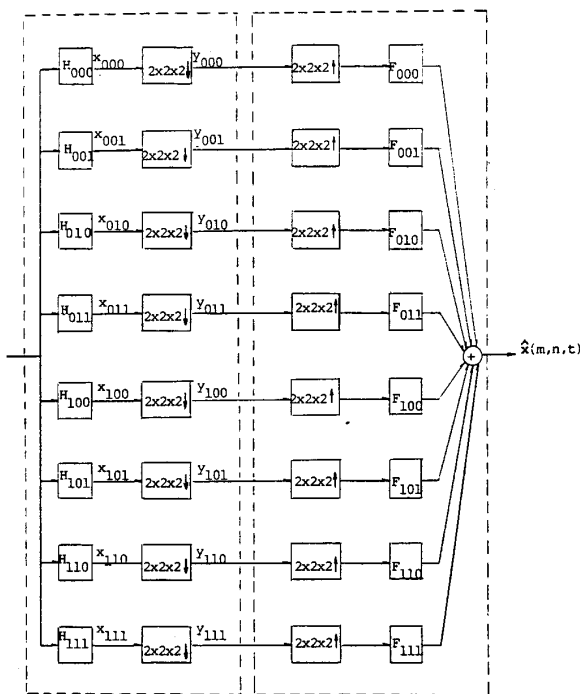


Fig. 2.

System Diagram of 3D Sub-band Coder With 8 Channel Analysis/Synthesis Filter Banks.

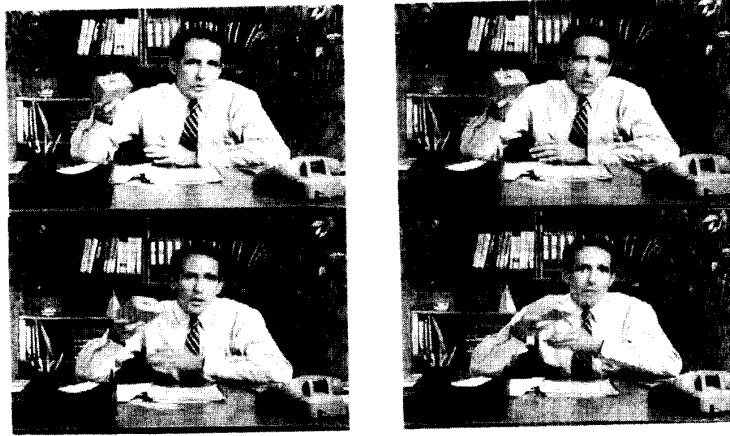
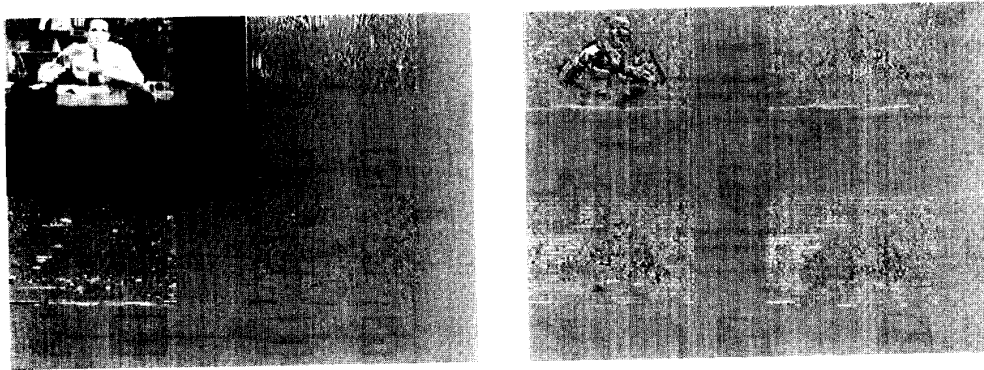


Fig. 4 The original image sequences : Salesman.



$$(c) \begin{array}{|c|c|} \hline y_{000}^{14}(m,n,t) & y_{100}^{14}(m,n,t) \\ \hline y_{010}^{14}(m,n,t) & y_{110}^{14}(m,n,t) \\ \hline \end{array} \quad (d) \begin{array}{|c|c|} \hline y_{001}^{14}(m,n,t) & y_{101}^{14}(m,n,t) \\ \hline y_{011}^{14}(m,n,t) & y_{111}^{14}(m,n,t) \\ \hline \end{array}$$

Fig. 5 3D spatiotemporal eight (4x2) subband image sequence decomposition by morphological filters. (a)(b) number 0 frame, (c)(d) number 14 frame.



$$(a) f_{00}^0(m,n,t) \quad (b) f_{10}^0(m,n,t).$$

Fig. 6 Image sequence synthesis by morphological eight (4x2) subband reconstruction method: four spatial subband synthesis images. (a) $f_{00}^0(m,n,t)$, (b) $f_{10}^0(m,n,t)$.

$$(a) f_{00}^0(m,n,t) \quad (b) f_{10}^0(m,n,t)$$

Fig. 7 Image sequence synthesis by morphological-eight (4x2) subband reconstruction method: (a) reconstructed image $\hat{x}^0(m,n,t)$, (b) error image $x^0(m,n,t) - \hat{x}^0(m,n,t)$.